ACS OMEGA

http://pubs.acs.org/journal/acsodf
Article

Selective Separation of Thiophene Derivatives Using Metal−Organic Frameworks-Based Membranes

Aigerim Ospanova,[‖] Kyran Kassym,[‖] Dana Kanzhigitova, Talgat Orazbek, Aida Ardakkyzy, Zhexenbek Toktarbay, and Nurxat Nuraje*

Cite This: *ACS Omega* 2024, 9, 42353−42360

ABSTRACT: The removal of sulfur compounds, particularly thiophene derivatives, from oil is crucial due to concerns about environmental issues. Therefore, the deep desulfurization of transportation fuels is currently an urgent problem, and numerous attempts have been made in this direction. Membrane-based desulfurization can be a good alternative to the traditional hydrodesulfurization method, which has several limitations. In this work, the use of membranes containing a metal−organic framework, MOF-5, doped with transition metals (Ag, Cu, Ni), in the adsorptive desulfurization process was studied. The efficiency of membranes was evaluated based on selective removal of thiophene and dibenzothiophene from model oil. Characterization techniques, including scanning electron microscopic (SEM), X-ray diffraction (XRD), Fourier transform infrared spectroscopy (FTIR), and thermogravimetric analysis (TGA), confirmed the successful synthesis and incorporation of metal−organic frameworks (MOFs) into mixed matrix membranes (MMMs). Desulfurization experiments showed that MOF-5/Ag exhibited the highest thiophene adsorption efficiency (86.8%), outperforming MOF-5/Cu and MOF-5/Ni. The enhanced performance is attributed to the strong interaction between silver and sulfur. These findings demonstrate the potential of MOF-based MMMs for efficient and selective desulfurization, offering a viable alternative to traditional hydrodesulfurization (HDS) methods.

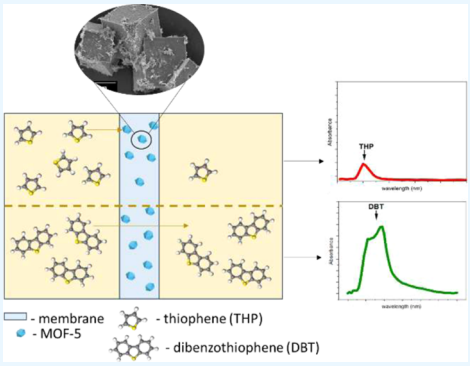

1. INTRODUCTION

Oil desulfurization is a critical step in the oil refining process due to stringent regulations on sulfur content in light and crude oil.[1] Sulfur impurities cause corrosion in refinery facilities and vehicle engines, and the combustion of sulfur-containing compounds in fuels releases toxic gases, such as sulfur dioxide (SO_2), which has detrimental environmental impacts. For instance, sulfur dioxide emissions contribute to acid rain, which causes significant damage to agricultural crops and poses health risks.[2] Therefore, treatment of pollution is significantly important today, as it addresses an urgent global problem that affects human health and well-being, and the sustainability of our planet's ecosystems.[3−5] Consequently, most countries have restricted sulfur levels in oil products to less than 10 ppm, with regulations becoming increasingly stringent.[6]

The most common industrial desulfurization technique is hydrodesulfurization (HDS), which converts sulfur compounds into hydrogen sulfide (H_2S) under high pressure and temperature conditions (300−400 °C).[7,8] However, HDS has several disadvantages, including high hydrogen consumption, limited catalyst life span, reduced octane numbers due to alkene saturation, and inefficiency in removing thiophene and its derivatives.[9,10] Approximately 80% of sulfur compounds in oil consist of thiophene and its derivatives, such as benzothiophene and dibenzothiophene, which are challenging to remove using HDS. These limitations result in low efficiency and high costs.[6]

Alternative desulfurization methods, such as alkylation, selective extraction, desulfurization with ionic liquids, and pervaporative desulfurization techniques, have emerged.[11−13] Among these, adsorptive desulfurization (ADS) has gained considerable attention due to its operation under ambient conditions (temperature and pressure) and the absence of hydrogen treatment required in HDS.[7] The key factor in ADS is the selection of materials for adsorbing sulfur compounds. Commonly used materials include activated carbon, zeolites, mesoporous silica, and alumina.

Metal−organic frameworks (MOFs) are highly versatile materials that have gained significant attention due to their unique properties and wide range of applications. MOFs are crystalline structures composed of metal ions or clusters coordinated to organic ligands, creating porous networks with

Received: June 12, 2024
Revised: August 24, 2024
Accepted: August 28, 2024
Published: September 10, 2024

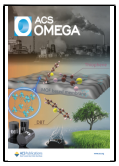

https://doi.org/10.1021/acsomega.4c05506
ACS Omega 2024, 9, 42353−42360

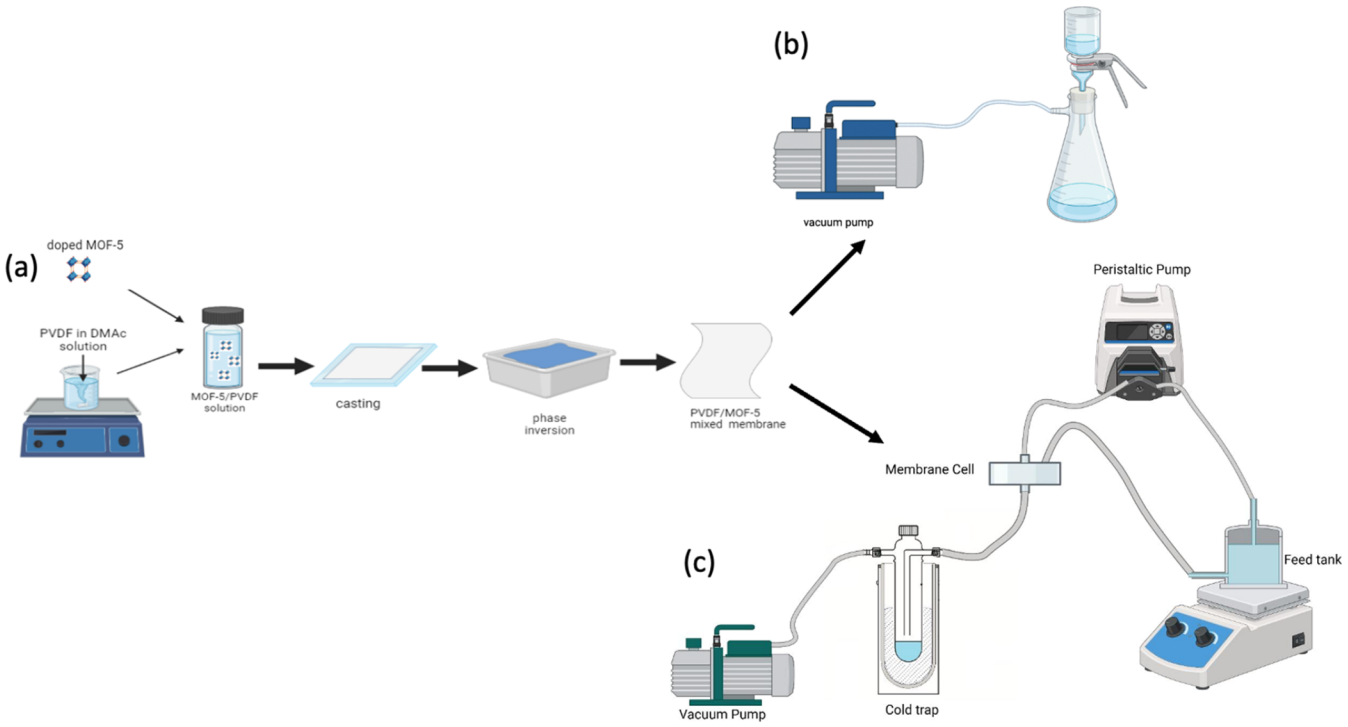

Figure 1. Flowchart of the process: (a) membrane preparation; (b) diagram of adsorptive filtration; (c) diagram of the pervaporation setup.

high surface areas.[14] Their tunable porosity and functional diversity make them ideal for advanced applications in different fields, such as biomedical, drug delivery,[15] catalysis,[16,17] environmental sustainability,[18] and energy storage.[19]

Moreover, MOFs have emerged as promising adsorbent materials for ADS due to their unique physical and chemical properties, such as high porosity, large surface area, and the presence of active sites.[20−22] MOFs also exhibit better compatibility with polymer matrices compared to other adsorbents like silica and carbon.[23−26] In recent years, some work has been conducted on improving the desulfurization capability of the ADS. The porosity and pore volume of MOFs have been demonstrated to be critical factors in determining their efficacy and functionality in a variety of applications, including adsorption and separation processes.[27] Therefore, various strategies, including Lewis-base interactions, hydrogen bonding, van der Waals forces, coordination, and π-complexation, have been employed to improve desulfurization performance.[21,28] Recent studies have shown that unsaturated coordinated metal sites are essential for deep desulfurization, and bimetallic Zn/Cu-BTC frameworks exhibit synergistic effects, leading to better desulfurization performance than monometallic Cu-BTC.[29]

Despite these advancements, limited research has been conducted on separating thiophene and its derivatives from model oils. So far, Ban et al. performed molecular modeling for the adsorption of thiophene, toluene, and isooctane on Ag-Cu-BTC and confirmed that thiophene has preferential adsorption with the assistance of silver dopants.[24] Therefore, it is worthwhile to study the separation of thiophene and its derivatives on their selective desulfurization using metal−organic frameworks. In this study, MOF-5 was chosen to examine the adsorption mechanism of thiophene (5 Å) and dibenzothiophene (8 Å) since it has a pore size of 1−2 nm.[30] Transition metals (Ag, Cu, and Ni) were selected to provide active sites on the surface of the adsorbent materials. The separation of thiophene (THP) and dibenzothiophene (DBT) in octane solutions was studied by designing bimetallic active sites within the MOF-5 membranes.

2. EXPERIMENTAL SECTION

2.1. Materials. All chemicals, including terephthalic acid ($C_6H_4(CO_2H)_2$), zinc acetate dihydrate ($Zn(OAc)_2{\cdot}2H_2O$), triethylamine ($(C_2H_5)_3N$), dimethylformamide (DMF), copper chloride ($CuCl_2$), silver nitrate ($AgNO_3$), nickel nitrate ($Ni(NO_3)_2$), poly(vinylidene fluoride) (PVDF), and *N*,*N*-dimethylacetamide (DMAC), were obtained from Sigma-Aldrich and used as received. All materials were used without further purification.

2.2. Synthesis of MOF-5. The synthesis of MOF-5 followed a method described in the literature.[26,31] Initially, 5.065 g (30.5 mmol) of terephthalic acid and 8.5 mL of triethylamine were dissolved in 400 mL of DMF. Separately, 16.99 g (77.4 mmol) of $Zn(OAc)_2{\cdot}2H_2O$ was dissolved in 500 mL of DMF. The zinc solution was added dropwise to the terephthalic acid solution under vigorous stirring. After the formation of a white precipitate, the mixture was stirred for 2.5 h. The precipitate was then centrifuged and soaked in DMF overnight. Subsequently, DMF was exchanged with $CHCl_3$ three times over 7 days. Finally, the product was dried in a vacuum oven overnight.

2.3. Doping of MOF-5 with Different Transition Metals. Doping of MOF-5 was conducted in a tube furnace via mixing with $CuCl_2$, $AgNO_3$, and $Ni(NO_3)_2$, respectively.[32] The above three different salts were, respectively, mixed with MOF-5 at a ratio of 3 mmol per gram. Then, the mixture was placed in a tube furnace and heated to 400 °C in a nitrogen atmosphere for 2h. The resulting materials were labeled as MOF-5/Cu, MOF-5/Ag and MOF-5/Ni.

2.4. Membrane Fabrication. Poly(vinylidene fluoride) (PVDF) was used as the polymer matrix for preparing mixed

https://doi.org/10.1021/acsomega.4c05506
ACS Omega 2024, 9, 42353−42360

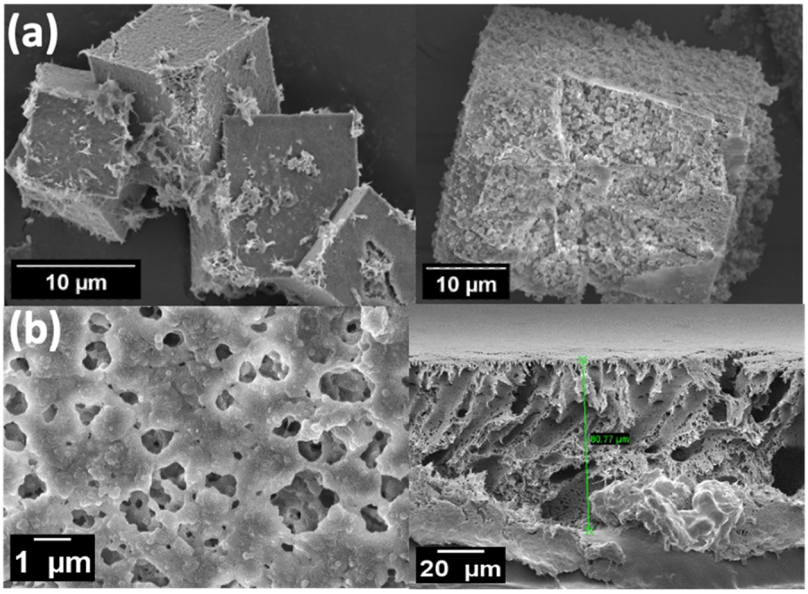

Figure 2. (a) SEM images of MOF-5. (b) SEM images of the PVDF/MOF-5/Ag membrane top view and cross section.

matrix membranes. PVDF was chosen for its excellent chemical resistance, thermal stability, and mechanical properties, making it suitable for polymer matrix in various advanced material applications.[33−35] PVDF's compatibility with metal−organic frameworks (MOFs) ensures the effective dispersion and retention of MOFs' properties in the mixed matrix membranes.

First, a 10 wt % PVDF solution in DMAC was prepared. Subsequently, 30 wt % (0.3 g) of MOF-5/Cu was dispersed in 10 mL of the PVDF solution using ultrasonication. This mixture was then cast onto a clean glass plate and immersed in a nonsolvent bath with distilled water for phase inversion.[36] Within a few minutes, a polymer film formed, which was then washed with distilled water and dried. The scheme of this method is illustrated in Figure 1a. Membranes with MOF-5/Ag and MOF-5/Ni were prepared similarly.

2.5. Desulfurization Experiments. Thiophene (THP, 3%), dibenzothiophene (DBT, 1%), and octane mixture was used as a model oil to perform desulfurization tests.

2.5.1. Adsorption. Separation was carried out using a funnel and vacuum pump; 10 mL of solution was poured on the membrane. The solution that passed through the filter was collected and the results were analyzed. A diagram of the process is shown in Figure 1b.

2.5.2. Pervaporation. As illustrated in Figure 1c, the feed solution was heated and circulated from the feed tank through the upstream side of the membrane cell using an adjustable flow rate pump. To minimize the influence of concentration polarization on the pervaporation performance, a high feed flow rate and an annular feed chamber were employed. The feed tank was heated to 70 °C, and the feed pump was set to a flow rate of 50 mL/min. The vacuum pump was turned on after the liquid began to reflux, maintaining a vacuum pressure of −1 bar. The pervaporation process was conducted for 30 min.

2.6. Characterization and Measurement. The morphology of MOF-5, membranes' top surface, and cross-sectional morphology were studied via scanning electron microscopic (SEM) (ZEISS Crossbeam 540). Before SEM observations were performed, each sample was fixed on a support using carbon tape and gold-sputtered. To cut the cross section of the membranes, they were frozen in advance with liquid nitrogen. Energy-dispersive X-ray spectroscopy (EDX) along with SEM was used to perform elemental mapping of MOF-5s. XRD System (SmartLab (Rigaku) Cu Kα radiation, λ = 1.5406 Å) was used to check the crystallographic properties and the formation of transition metals such as Ag, Cu, and Ni. Using Fourier transform infrared spectroscopy (Nicolet iS10 FT-IR spectrometer), the chemical structures of the MOF-5 and doped MOF-5s have been studied. CHNS elemental analysis (UNICUBE trace Organic Elemental Analyzer) was conducted to confirm that membranes absorb THP. Thermogravimetric analysis [Simultaneous Thermal Analyzer (STA) 6000] was performed to study the thermal properties of composite materials.

The efficiency of the desulfurization process was defined by a decrease in sulfur compounds concentration. The concentration was measured using the ultrahigh-performance liquid chromatography (UHPLC UltiMate 3000) method. For this purpose, 9 standard solutions of THP and DBT in octane with different concentrations were prepared, and their retention time was measured. Calibration curves are provided in Figure S1.

3. RESULTS AND DISCUSSION

The aim of this research is to study the adsorption of thiophene and its derivatives in octane solution using metal−organic framework (MOF-5) composites for the first time. To test the selective adsorption of THP over DBT based on the hypothesis that binary active sites create different binding affinities for thiophene and its derivatives and affect the pore size (one of the crucial parameters), MOF-5 [with a pore size of 1−2 nm (Figure S2)] was chosen to fabricate the three different MOF-5 modified composite membranes doped with transition metals such as Cu, Ag, and Ni. Three different model systems—THP/octane, DBT/octane, and THP/DBT/octane—were selected to study adsorption on PVDF composite membranes consisting of PVDF/MOF-5 modified by Cu, Ag, and Ni. Subsequently, the three different composite membranes were tested for adsorption of the three different model fluids.

https://doi.org/10.1021/acsomega.4c05506
ACS Omega 2024, 9, 42353−42360

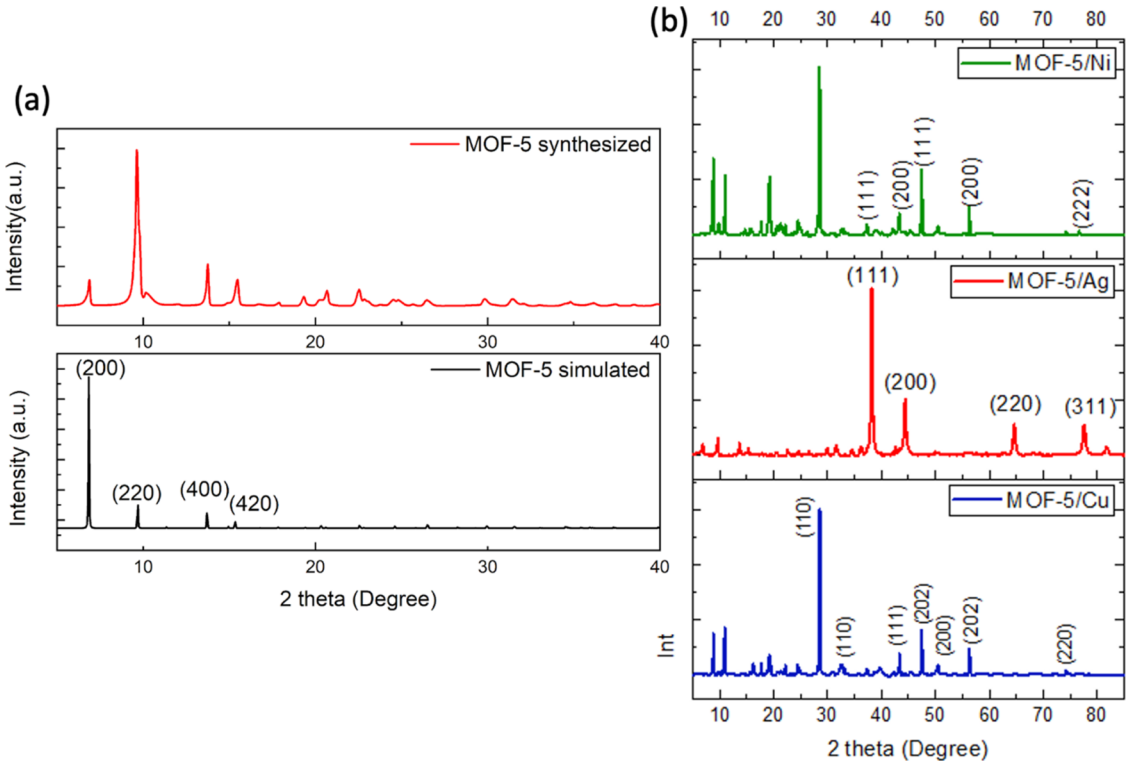

Figure 3. (a) XRD pattern of MOF-5. (b) XRD patterns of MOF-5/Ag, MOF-5/Cu, and MOF-5/Ni.

3.1. Characterization of MOF-5/Ag, MOF-5/Cu, and MOF-5/Ni. The morphology of the MOF-5 synthesized is shown in Figure 2. The MOF-5 has a clearly defined cubic crystal structure with particle sizes ranging from 10 to 40 μm. Therefore, MOF-5 was synthesized as shown in Figure 2a. The porous structure of the PVDF/MOF-5/Ag membrane can be observed in Figure 2b.

Figure 3a displays the experimentally obtained XRD graphs of the MOF-5 and XRD patterns from the database. The agreement between these patterns confirms the successful synthesis of MOF-5 and its highly crystalline structure. However, the intensities of the first two peaks, 2θ = 6.9 and 9.7°, are inverted, likely due to modifications in atomic orientations in the crystal planes caused by adsorbed species (solvent and water molecules).[37,38]

Figure 3b shows the XRD spectra of the MOF-5 doped with different transition metals. The crystalline characters of the products are evident with sharp peaks similar to those of pure MOF-5, alongside additional peaks or variations indicative of metal incorporation. Strong diffraction peaks at 2θ = 38.15, 44.35, 64.5, and 77.45° correspond to the (111), (200), (220), and (311) crystal planes of Ag, respectively. Peaks at 2θ = 43.35, 50.5, and 74.5° correspond to the (111), (200) and (220) planes of Cu; 2θ = 29, 32.5, 47.7, 53.6, and 56.5° correspond to the (110), (110), (202), (020), and (202) planes of CuO, respectively. Peaks at 2θ = 47.5, 56.3, and 76.4° match the (111), (200), and (220) planes of Ni; 2θ = 37.2, 43.2° match the (111) and (200) planes of NiO.

Results of the EDS analysis are summarized in Table 1. These elemental analysis results show that all three samples contain the expected elements (Ag, Cu, and Ni) alongside the elements from the MOF-5 structure itself (Zn, C, and O). The presence of peaks for Ag, Cu, and Ni confirms the successful doping process with the desired transition metals. The MOF-5

Table 1. Elemental Composition of Doped MOF-5

MOF-5/Ag		MOF-5/Cu		MOF-5/Ni	
elements	wt %	elements	wt %	elements	wt %
Zn	12.3	Zn	23.6	Zn	37.1
C	4.7	C	37.7	C	26.9
O	4.2	O	13.8	O	12.2
Ag	78.2	Cu	17.9	Ni	23.8
		Cl	7.0		

was separately modified with $CuCl_2$, $AgNO_3$, and $Ni(NO_3)_2$ using tube furnace equipment to create MOF-5/Cu, MOF-5/Ag, and MOF-5/Ni. Subsequently, PVDF/MOF-5/Cu, PVDF/MOF-5/Ag, and PVDF/MOF-5/Ni mixed matrix membranes were produced via the casting approach (Figure 1a). Figure S3 displays the key FTIR peaks corresponding to carboxylate groups, aromatic rings, and metal−oxygen interactions. There are two main peaks at 1380 and 1597 cm^{-1} indicating the attachment of carboxylate groups to the Zn4O center. The absorption peak at 745 cm^{-1} is associated with the stretching mode of Zn−O inside the Zn4O lattice complex in MOF-5. Shifts and changes in key peaks, particularly those related to carboxylate groups and the fingerprint region, indicate the successful incorporation of Ag, Cu, and Ni into the MOF-5 matrix.

The thermal stability of membranes and amount of MOFs added into PVDF matrix was evaluated using a thermogravimetric analysis (TGA) method (Figure 4). Here, in the enlarged view, one can see that the PVDF membrane started deteriorating around the temperature range of ca. 420−440 °C. In contrast, the mixed matrix membranes (PVDF/MOF-5/Ag, PVDF/MOF-5/Cu, and PVDF/MOF-5/Ni) began decomposing earlier around the temperature of ∼350 °C. However, the most significant weight loss was shifted to higher

https://doi.org/10.1021/acsomega.4c05506
ACS Omega 2024, 9, 42353−42360

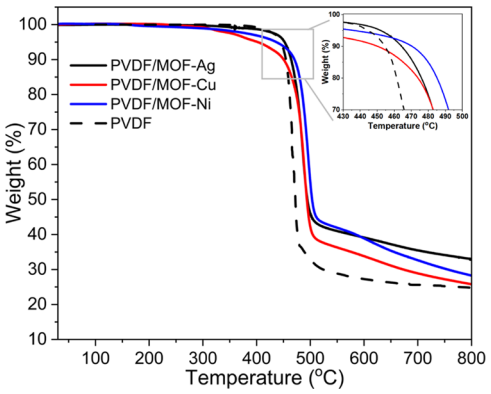

Figure 4. TGA of PVDF and mixed matrix membranes.

temperatures, meaning that in the presence of MOF particles, the thermal stability of PVDF was improved. The slower degradation for mixed matrix membranes might indicate a strong interaction of fillers with polymer matrix that leads to a higher thermal stability. The residual masses of membranes were around 33, 28.5, and 25% for MOF-5/Ag, MOF-5/Ni, and MOF-5/Cu, respectively, which corresponds to the initially added 30 wt % MOFs.[39−41]

3.2. Desulfurization Results. The results of desulfurization for the three different membranes consisting of MOF-5/Ag, MOF-5/Cu, and MOF-5/Ni from the adsorption desulfurization experiments are presented in the following figures. Figure 5 shows the THP removal efficiency, with

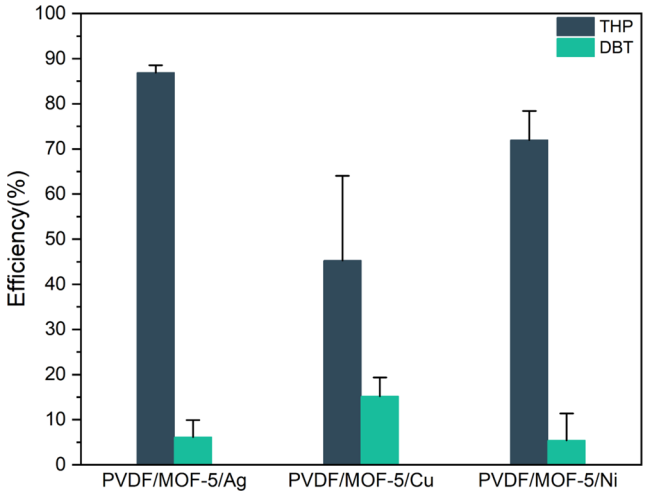

Figure 5. Thiophene and dibenzothiophene removal efficiency of MOF-5/Ag, MOF-5/Cu, and MOF-5/Ni.

MOF-5/Ag having the highest removal efficiency of 86.8%. However, the efficiencies of membranes with MOF-5/Cu and MOF-5/Ni are 45.24 and 71.96%, respectively. The best separation performance for the membrane with MOF-5/Ag can be explained by the strong interaction between silver and sulfur compared to that of other metals. In addition, both MOF-5/Cu and MOF-5/Ni in the composite membranes contain a mixture of metal and metal oxides, unlike the case for MOF-5/Ag. However, all three membranes have low efficiency in the removal of DBT.

The adsorption experiments indicated that the membranes doped with three different metals were more effective in removing THP than DBT, indicating a selective character toward THP. This selectivity can be attributed to several mechanisms, as illustrated in Figure 6.

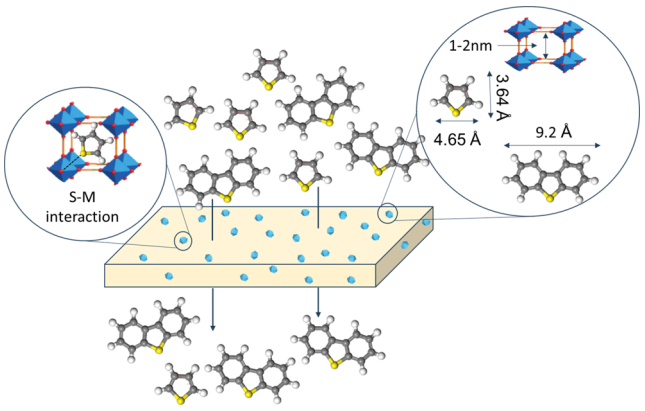

Figure 6. Schematic illustration for possible adsorption mechanism of thiophene and dibenzothiophene toward the MOF-modified composite membranes.

Thiophene easily fits inside the pores of MOF-5s and interacts with the metal centers or functional groups because it is a smaller, more polar molecule with a lower molecular weight than DBT.[42] The pore size of MOF-5 was measured by nitrogen porosimeter, and the indicated material is mostly microporous (less than 2 nm) as shown in Figure S2. Based on the results of this study, the specific surface and pore size distribution have a great effect on the properties of the prepared composites and the prepared materials may be useful in other applications such as electromagnetic wave absorptions according to the study of similar works.[43,44]

Additionally, thiophene interacts with the MOF more readily than does DBT because it has a simpler molecular structure. The larger and less polar DBT molecule, on the other hand, may not fit easily into the pores of MOF-5 and may not interact with doped transition metals due to the steric hindrance. Through a single pair of electrons that may interact with transition metals through a sort of chemical bonding known as a sulfur−metal (S−M) interaction, thiophene is more easily able to connect with transition metals than DBT. This behavior is similar to how specific interactions can be influenced by surface properties and chemical environments, as discussed in the context of the interaction between silane and organic molecules.[45,46] As a result of the surrounding aromatic rings, the sulfur atom may be less accessible to the metals, making it more challenging for DBT to react with transition metals through an S−M interaction due to the steric hindrance effect. Due to DBT's larger size and more complicated structure, the distance between the sulfur atom and the metals may also be greater, which can weaken the S−M interaction even more.

According to Pearson's classification, Cu and Ni are considered borderline acids, while Ag is classified as a soft acid.[47] The hard−soft acid−base theory suggests that soft acids have a stronger interaction with soft bases. Consequently, the interaction between thiophene and Ag is stronger than that with Cu or Ni. This explains why MOF-5/Ag demonstrates a higher removal efficiency compared to that of MOF-5/Cu and MOF-5/Ni.

CHNS elemental analysis was further performed to investigate the adsorption behaviors of both THP and DBT

https://doi.org/10.1021/acsomega.4c05506
ACS Omega 2024, 9, 42353−42360

on the above membranes with doped metals before and after separation processes. The result indicated no presence of DBT in the membrane which is opposite to THP adsorption (Table S1). From Figure 6, it is clear that sulfur content after separation of thiophene increased much more than that of DBT. Therefore, it can be assumed that DBT passed through the membrane without having significant interaction with metal-doped MOF-5 in the membrane.

To double confirm the obtained results from the adsorption experimental setup, a pervaporation method was used to test the desulfurization performance of the composite membranes as shown in Figure 1c. The results (Figure 7) from the

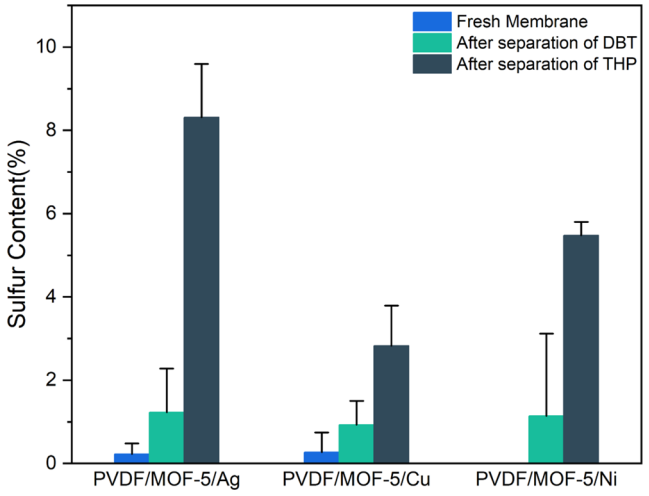

Figure 7. Sulfur content in fresh membranes after separation of DBT and after separation of THP.

pervaporation model are consistent with adsorptive filtration, showing that PVDF/MOF-5/Ag has the best ability to remove thiophene. These results also have a similar trend in selectivity for thiophene rather than DBT.

However, the efficiency of the membranes in the pervaporation setup is lower than that in the adsorption filtration test. It may be caused by the fact that conducting the filtration experiments in an open system could lead to some solution evaporation caused by the operation of the vacuum pump. This potential evaporation could result in data inaccuracies. In contrast, the pervaporation model allows for the provision of desulfurization samples to the membrane in a closed environment by using a heated reflux system (Figure 8).

4. CONCLUSIONS

This work focuses on the design and fabrication of polymer nanocomposite membranes for adsorptive oil desulfurization and the investigation of the structure−property relationship for selective adsorption of THP and DBT from octane. MOF-5 with an average size of 10−40 μm and pore size of 1−2 nm were synthesized, further doped with Ag, Cu, and Ni transition metals, and were embedded into the PVDF matrix to fabricate their composite membranes. The desulfurization efficiency of membranes was studied via the adsorption model and double-confirmed using the pervaporation model.

It was observed that THP interacts more readily with the doped MOF-5s inside of MMMs compared to DBT. This is attributed to the simpler molecular structure of THP, which allows for easier access and interaction with the transition

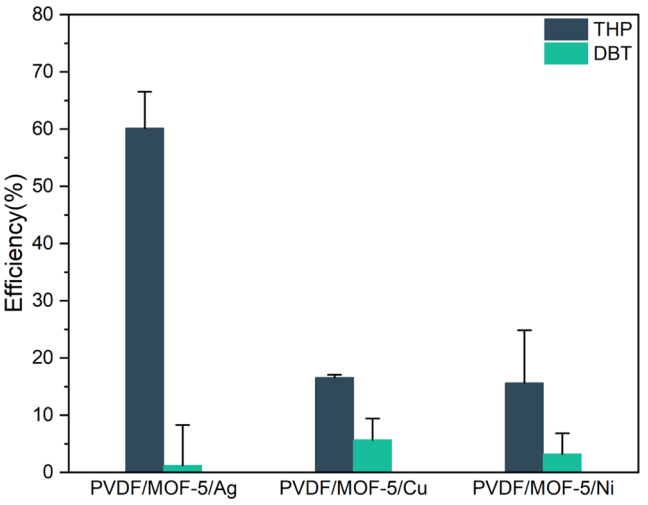

Figure 8. Pervaporation efficiencies of MOF-5/Ag, MOF-5/Cu, and MOF-5/Ni.

metals through sulfur−metal (S−M) interactions. The study examining the impact of various transition metals on the desulfurization performance of membranes revealed that PVDF/MOF-5/Ag demonstrated the highest removal of THP, significantly outperforming its copper and nickel counterparts. This performance can be attributed to the strong affinity between silver and sulfur, which facilitates the effective adsorption of sulfur compounds. Since silver is classified as a soft acid, it interacts more strongly with thiophene, which acts as a soft base, compared to the borderline acids copper and nickel.

In conclusion, the use of MOF-based MMMs, particularly those doped with silver, presents a promising approach for the selective adsorption of thiophene derivatives, contributing to cleaner fuel production and compliance with environmental regulations. Future research should focus on exploring the scalability of these membranes and evaluating their performance in real-world desulfurization applications.

■ ASSOCIATED CONTENT

Supporting Information

The Supporting Information is available free of charge at https://pubs.acs.org/doi/10.1021/acsomega.4c05506.

Calibration curve for THP and DBT BET data, FTIR spectra, and elemental composition analysis for MOF-modified membranes (PDF)

■ AUTHOR INFORMATION

Corresponding Author

Nurxat Nuraje − *Department of Chemical & Materials Engineering, School of Engineering & Digital Science, Nazarbayev University, Astana 010000, Kazakhstan; Renewable Energy Laboratory, National Laboratory Astana, Nazarbayev University, Astana 010000, Kazakhstan;* orcid.org/0000-0002-4335-8905; Email: nurxat.nuraje@nu.edu.kz

Authors

Aigerim Ospanova − *Department of Chemical & Materials Engineering, School of Engineering & Digital Science, Nazarbayev University, Astana 010000, Kazakhstan*

https://doi.org/10.1021/acsomega.4c05506
ACS Omega 2024, 9, 42353−42360

Kyran Kassym − *Department of Chemical & Materials Engineering, School of Engineering & Digital Science, Nazarbayev University, Astana 010000, Kazakhstan*
Dana Kanzhigitova − *Department of Chemical & Materials Engineering, School of Engineering & Digital Science, Nazarbayev University, Astana 010000, Kazakhstan; Renewable Energy Laboratory, National Laboratory Astana, Nazarbayev University, Astana 010000, Kazakhstan*
Talgat Orazbek − *Renewable Energy Laboratory, National Laboratory Astana, Nazarbayev University, Astana 010000, Kazakhstan*
Aida Ardakkyzy − *Department of Chemical & Materials Engineering, School of Engineering & Digital Science, Nazarbayev University, Astana 010000, Kazakhstan*
Zhexenbek Toktarbay − *Laboratory of Engineering Profile, Satbayev University, Almaty 050000, Kazakhstan*

Complete contact information is available at: https://pubs.acs.org/10.1021/acsomega.4c05506

Author Contributions

[‖]A.O. and K.K. contributed equally to this work. The manuscript was written through contributions of all authors. All authors have given approval to the final version of the manuscript.

Notes

The authors declare no competing financial interest.

■ ACKNOWLEDGMENTS

This work was supported by the Ministry of Education and Science of the Republic of Kazakhstan (grant nos. AP14871259 and BR21882439).

■ REFERENCES

(1) Stanislaus, A.; Marafi, A.; Rana, M. S. Recent Advances in the Science and Technology of Ultra Low Sulfur Diesel (ULSD) Production. *Catal. Today* **2010**, *153* (1−2), 1−68.
(2) Shammas, N. K.; Wang, L. K.; Wang, M.-H. S. Sources, Chemistry and Control of Acid Rain in the Environment. In *Handbook of Environment and Waste Management: Acid Rain and Greenhouse Gas Pollution Control*; World Scientific, 2020; Vol. 3, pp 1−26.
(3) Wu, Q.; Gao, L.; Huang, M.; Mersal, G. A. M.; Ibrahim, M. M.; El-Bahy, Z. M.; Shi, X.; Jiang, Q. Aminated Lignin by Ultrasonic Method with Enhanced Arsenic (V) Adsorption from Polluted Water. *Adv. Compos. Hybrid Mater.* **2022**, *5* (2), 1044−1053.
(4) Sun, Z.; Zhang, Y.; Guo, S.; Shi, J.; Shi, C.; Qu, K.; Qi, H.; Huang, Z.; Murugadoss, V.; Huang, M.; Guo, Z. Confining FeNi Nanoparticles in Biomass-Derived Carbon for Effectively Photo-Fenton Catalytic Reaction for Polluted Water Treatment. *Adv. Compos. Hybrid Mater.* **2022**, *5* (2), 1566−1581.
(5) Sun, J.; Mu, Q.; Kimura, H.; Murugadoss, V.; He, M.; Du, W.; Hou, C. Oxidative Degradation of Phenols and Substituted Phenols in the Water and Atmosphere: A Review. *Adv. Compos. Hybrid Mater.* **2022**, *5* (2), 627−640.
(6) Mitra, D. Desulfurization of Gasoline by Pervaporation. *Sep. Purif. Rev.* **2012**, *41* (2), 97−125.
(7) Saha, B.; Vedachalam, S.; Dalai, A. K. Review on Recent Advances in Adsorptive Desulfurization. *Fuel Process. Technol.* **2021**, *214*, No. 106685.
(8) Bello, S. S.; Wang, C.; Zhang, M.; Gao, H.; Han, Z.; Shi, L.; Su, F.; Xu, G. A Review on the Reaction Mechanism of Hydrodesulfurization and Hydrodenitrogenation in Heavy Oil Upgrading. *Energy Fuels* **2021**, *35* (14), 10998−11016.
(9) Sano, Y.; Sugahara, K.; Choi, K.; Korai, Y.; Mochida, I. Two-Step Adsorption Process for Deep Desulfurization of Diesel Oil. *Fuel* **2005**, *84* (7−8), 903−910.
(10) Zaidi, Z.; Gupta, Y.; Gayatri, S. L.; Singh, A. A Comprehensive Discussion on Fuel Combustion and Desulfurization Technologies. *Inorg. Chem. Commun.* **2023**, *154*, No. 110964.
(11) Chandra Srivastava, V. An Evaluation of Desulfurization Technologies for Sulfur Removal from Liquid Fuels. *RSC Adv.* **2012**, *2* (3), 759−783.
(12) Ospanova, A.; Ardakkyzy, A.; Kurbanova, A.; Kanagat, Y.; Abutalip, M.; Toktarbay, Z.; Nuraje, N. Pervaporative Desulfurization: A Comprehensive Review of Principles, Advances, and Applications. *Eurasian J. Chem.* **2023**, *112* (4), 112−122.
(13) Matus, EV.; Yashnik, S. A.; Salnikov, A. V.; Khitsova, L. M.; Popova, A. N.; Nikitin, A. P.; Sozinov, S. A.; Ismagilov, Z. R. Genesis and Properties of MOx/CNTs (M = Ce, Cu, Mo) Catalysts for Aerobic Oxidative Desulfurization of a Model Diesel Fuel. *Eurasian Chem.-Technol. J.* **2021**, *23* (4), 267.
(14) Zhou, H.-C.; Kitagawa, S. Metal−Organic Frameworks (MOFs). *Chem. Soc. Rev.* **2014**, *43* (16), 5415−5418.
(15) Rahaman, S. J.; Samanta, A.; Mir, M. H.; Dutta, B. Metal-Organic Frameworks (MOFs): A Promising Candidate for Stimuli-Responsive Drug Delivery. *ES Mater. Manuf.* **2022**, *7* (1), No. 4.
(16) Bag, P. P.; Singh, G. P.; Singha, S.; Roymahapatra, G. Synthesis of Metal-Organic Frameworks (MOFs) and Their Applications to Biology, Catalysis and Electrochemical Charge Storage: A Mini Review. *Eng. Sci.* **2020**, *13*, 1−10.
(17) Iniyan, S.; Ren, J.; Deshmukh, S.; Rajeswaran, K.; Jegan, G.; Hou, H.; Suryanarayanan, V.; Murugadoss, V.; Kathiresan, M.; Xu, B. B.; Guo, Z. An Overview of Metal-Organic Framework Based Electrocatalysts: Design and Synthesis for Electrochemical Hydrogen Evolution, Oxygen Evolution, and Carbon Dioxide Reduction Reactions. *Chem. Rec.* **2023**, *23* (12), No. e202300317.
(18) Du, Z.; Chen, F.; Fang, S.; Yang, X.; Ge, Y.; Shurtz, K.; Zhou, H.-C.; Hu, Y. H.; Li, Y. Engineering Bimetallic Ni-Cu Nanoparticles Confined in MOF-Derived Nanocomposite for Efficient Dry Reforming of Methane. *ES Energy Environ.* **2024**, *23*, No. 1097.
(19) Acharya, D.; Ko, T. H.; Bhattarai, R. M.; Muthurasu, A.; Kim, T.; Saidin, S.; Choi, J.-S.; Chhetri, K.; Kim, H. Y. Double-Phase Engineering of Cobalt Sulfide/Oxyhydroxide on Metal-Organic Frameworks Derived Iron Carbide-Integrated Porous Carbon Nanofibers for Asymmetric Supercapacitors. *Adv. Compos. Hybrid Mater.* **2023**, *6* (5), 179.
(20) Kampouraki, Z.-C.; Giannakoudakis, D. A.; Nair, V.; Hosseini-Bandegharaei, A.; Colmenares, J. C.; Deliyanni, E. A. Metal Organic Frameworks as Desulfurization Adsorbents of DBT and 4,6-DMDBT from Fuels. *Molecules* **2019**, *24* (24), 4525.
(21) Khan, N. A.; Hasan, Z.; Jhung, S. H. Adsorptive Removal of Hazardous Materials Using Metal-Organic Frameworks (MOFs): A Review. *J. Hazard. Mater.* **2013**, *244*−*245*, 444−456.
(22) Peralta, D.; Chaplais, G.; Simon-Masseron, A.; Barthelet, K.; Pirngruber, G. D. Metal−Organic Framework Materials for Desulfurization by Adsorption. *Energy Fuels* **2012**, *26* (8), 4953−4960.
(23) Furukawa, H.; Cordova, K. E.; O'Keeffe, M.; Yaghi, O. M. The Chemistry and Applications of Metal-Organic Frameworks. *Science* **2013**, *341* (6149), No. 1230444.
(24) Ban, S.; Long, K.; Xie, J.; Sun, H.; Zhou, H. Thiophene Separation with Silver-Doped Cu-BTC Metal−Organic Framework for Deep Desulfurization. *Ind. Eng. Chem. Res.* **2018**, *57* (8), 2956−2966.
(25) Zhang, Y.; Song, J.; Pan, F.; Li, Y.; Zhao, J.; Wang, S.; Huang, Y.; Li, Y.; Jiang, Z. Constructing High-Efficiency Facilitated Transport Pathways via Embedding Heterostructured Ag+@MOF/GO Laminates into Membranes for Pervaporative Desulfurization. *Sep. Purif. Technol.* **2020**, *245*, No. 116858.
(26) Tranchemontagne, D. J.; Hunt, J. R.; Yaghi, O. M. Room Temperature Synthesis of Metal-Organic Frameworks: MOF-5,

MOF-74, MOF-177, MOF-199, and IRMOF-0. *Tetrahedron* **2008**, *64* (36), 8553−8557.
(27) Baumann, A. E.; Burns, D. A.; Liu, B.; Thoi, V. S. Metal-Organic Framework Functionalization and Design Strategies for Advanced Electrochemical Energy Storage Devices. *Commun. Chem.* **2019**, *2* (1), 86.
(28) Ahmed, I.; Jhung, S. H. Adsorptive Desulfurization and Denitrogenation Using Metal-Organic Frameworks. *J. Hazard. Mater.* **2016**, *301*, 259−276.
(29) Wang, T.; Li, X.; Dai, W.; Fang, Y.; Huang, H. Enhanced Adsorption of Dibenzothiophene with Zinc/Copper-Based Metal−Organic Frameworks. *J. Mater. Chem. A* **2015**, *3* (42), 21044−21050.
(30) Fei, L.; Rui, J.; Wang, R.; Lu, Y.; Yang, X. Equilibrium and Kinetic Studies on the Adsorption of Thiophene and Benzothiophene onto NiCeY Zeolites. *RSC Adv.* **2017**, *7* (37), 23011−23020.
(31) Biserčić, M. S.; Marjanović, B.; Vasiljević, B. N.; Mentus, S.; Zasońska, B. A.; Ćirić-Marjanović, G. The Quest for Optimal Water Quantity in the Synthesis of Metal-Organic Framework MOF-5. *Microporous Mesoporous Mater.* **2019**, *278*, 23−29.
(32) Dai, W.; Zhou, Y.; Li, S.; Li, W.; Su, W.; Sun, Y.; Zhou, L. Thiophene Capture with Complex Adsorbent SBA-15/Cu(I). *Ind. Eng. Chem. Res.* **2006**, *45* (23), 7892−7896.
(33) Wang, Y.; Yang, D.; Hessien, M. M.; Du, K.; Ibrahim, M. M.; Su, Y.; Mersal, G. A. M.; Ma, R.; El-Bahy, S. M.; Huang, M.; Yuan, Q.; Cui, B.; Hu, D. Flexible Barium Titanate@polydopamine/Polyvinylidene Fluoride/Polymethyl Methacrylate Nanocomposite Films with High Performance Energy Storage. *Adv Compos. Hybrid Mater.* **2022**, *5* (3), 2106−2115.
(34) Sharafkhani, S.; Kokabi, M. Enhanced Sensing Performance of Polyvinylidene Fluoride Nanofibers Containing Preferred Oriented Carbon Nanotubes. *Adv Compos. Hybrid Mater.* **2022**, *5* (4), 3081−3093.
(35) Wu, Z.; Wang, X.; Annamareddy, S. H. K.; Gao, S.; Xu, Q.; Algadi, H.; Sridhar, D.; Wasnik, P.; Xu, B. Bin.; Weng, L.; Guo, Z. Dielectric Properties and Thermal Conductivity of Polyvinylidene Fluoride Synergistically Enhanced with Silica@Multi-Walled Carbon Nanotubes and Boron Nitride. *ES Mater. Manuf.* **2023**, *22*, No. 847.
(36) Ding, H.; Pan, F.; Mulalic, E.; Gomaa, H.; Li, W.; Yang, H.; Wu, H.; Jiang, Z.; Wang, B.; Cao, X.; Zhang, P. Enhanced Desulfurization Performance and Stability of Pebax Membrane by Incorporating Cu+ and Fe2+ Ions Co-Impregnated Carbon Nitride. *J. Membr. Sci.* **2017**, *526*, 94−105.
(37) Hafizovic, J.; Bjørgen, M.; Olsbye, U.; Dietzel, P. D. C.; Bordiga, S.; Prestipino, C.; Lamberti, C.; Lillerud, K. P. The Inconsistency in Adsorption Properties and Powder XRD Data of MOF-5 Is Rationalized by Framework Interpenetration and the Presence of Organic and Inorganic Species in the Nanocavities. *J. Am. Chem. Soc.* **2007**, *129* (12), 3612−3620.
(38) Ata-ur-Rehman; Tirmizi, S. A.; Badshah, A.; Ammad, H. M.; Jawad, M.; Abbas, S. M.; Rana, U. A.; Khan, S. U.-D. Synthesis of Highly Stable MOF-5@MWCNTs Nanocomposite with Improved Hydrophobic Properties. *Arab. J. Chem.* **2018**, *11* (1), 26−33.
(39) Caparros, C.; Lopes, A. C.; Ferdov, S.; Lanceros-Mendez, S. γ-Phase Nucleation and Electrical Response of Poly(Vinylidene Fluoride)/Microporous Titanosilicates Composites. *Mater. Chem. Phys.* **2013**, *138* (2−3), 553−558.
(40) Cao, X. T.; Vo, T. K.; An, T. N. M.; Nguyen, T. D.; Kabtamu, D. M.; Kumar, S. Enhanced Dye Adsorption of Mixed-Matrix Membrane by Covalent Incorporation of Metal-Organic Framework with Poly(Styrene-*Alt*-maleic Anhydride). *ChemistrySelect* **2021**, *6* (19), 4689−4697.
(41) Kim, M.; Wu, Y. S.; Kan, E. C.; Fan, J. Breathable and Flexible Piezoelectric ZnO@PVDF Fibrous Nanogenerator for Wearable Applications. *Polymers* **2018**, *10* (7), 745.
(42) Li, Y.-X.; Jiang, W.-J.; Tan, P.; Liu, X.-Q.; Zhang, D.-Y.; Sun, L.-B. What Matters to the Adsorptive Desulfurization Performance of Metal−Organic Frameworks? *J. Phys. Chem. C* **2015**, *119* (38), 21969−21977.
(43) Li, F.; Wu, N.; Kimura, H.; Wang, Y.; Xu, B. B.; Wang, D.; Li, Y.; Algadi, H.; Guo, Z.; Du, W.; Hou, C. Initiating Binary Metal Oxides Microcubes Electromagnetic Wave Absorber Toward Ultrabroad Absorption Bandwidth Through Interfacial and Defects Modulation. *Nanomicro Lett.* **2023**, *15* (1), 220.
(44) Li, F.; Bi, Z.; Kimura, H.; Li, H.; Liu, L.; Xie, X.; Zhang, X.; Wang, J.; Sun, X.; Ma, Z.; Du, W.; Hou, C. Energy- and Cost-Efficient Salt-Assisted Synthesis of Nitrogen-Doped Porous Carbon Matrix Decorated with Nickel Nanoparticles for Superior Electromagnetic Wave Absorption. *Adv. Compos. Hybrid Mater.* **2023**, *6* (4), 133.
(45) Suiindik, Z.; Adotey, E.; Kydyrbay, N.; Zhazitov, M.; Nuraje, N.; Toktarbaiuly, O. Formulating Superhydrophobic Coatings with Silane for Microfiber Applications. *Eurasian Chem.-Technol. J.* **2024**, *26* (2), 53−60.
(46) Toktarbaiuly, O.; Kurbanova, A.; Imekova, G.; Abutalip, M.; Toktarbay, Z. Desert Water Saving and Transportation for Enhanced Oil Recovery: Bridging the Gap for Sustainable Oil Recovery. *Eurasian Chem.-Technol. J.* **2023**, *25* (3), 193−200.
(47) Pearson, R. G. Hard and Soft Acids and Bases. *J. Am. Chem. Soc.* **1963**, *85* (22), 3533−3539.

https://doi.org/10.1021/acsomega.4c05506
ACS Omega 2024, 9, 42353−42360